Journal of Molecular Structure 990 (2011) 158–163

Contents lists available at ScienceDirect

Journal of Molecular Structure

journal homepage: www.elsevier.com/locate/molstruc

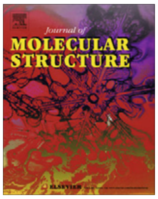

Aminobenzonitrile isomers-mediated self-assembly of mixed-ligand silver(I) coordination architectures: Synthesis, structural characterization and properties

Fu-Jing Liu [a], Di Sun [a], Yun-Hua Li [a], Hong-Jun Hao [a], Geng-Geng Luo [b], Rong-Bin Huang [a,*], Lan-Sun Zheng [a]

[a] *State Key Laboratory for Physical Chemistry of Solid Surfaces and Department of Chemistry, College of Chemistry and Chemical Engineering, Xiamen University, Xiamen, 361005, China*
[b] *Institute of Materials Physical Chemistry, Huaqiao University, Xiamen, Fujian 361021, China*

ARTICLE INFO

Article history:
Received 12 January 2011
Received in revised form 20 January 2011
Accepted 20 January 2011
Available online 26 January 2011

Keywords:
Silver(I)
Aminobenzonitrile ligand
3,5-Dinitrobenzoic acid
Ag···Ag interaction
Photoluminescence

ABSTRACT

Three mixed-ligand coordination compounds (CCs) of the formula $\{[Ag(p\text{-abn})(dnca)]\cdot H_2O\}_n$ (**1**), $\{[Ag(o\text{-abn})(dnca)]\cdot H_2O\}_n$ (**2**), and $\{[Ag(m\text{-abn})_4)]\cdot(dnca)\cdot H_2O\}$ (**3**) (where *p*-abn = 4-aminobenzonitrile, *o*-abn = 2-aminobenzonitrile, *m*-abn = 3-aminobenzonitrile, Hdnca = 3,5-dinitrobenzoic acid) were synthesized by reactions of Ag_2O and aminobenzonitrile ligands with Hdnca under the ammoniacal condition. All CCs have been structurally characterized by element analysis, IR and X-ray single-crystal diffraction. The aminobenzonitrile acts as bidentate μ_2-*N,N′* ligand in both **1** and **2**, and as monodentate ligand in **3**. As the change of the relative position of amino and cyano groups of aminobenzonitrile ligands, the dimensionality of **1–3** decreases from 2D to 0D mainly due to the steric effect of the substituted groups, which indicates that aminobenzonitrile isomers play important roles in the formation of the diverse coordination architectures. The three CCs exhibit photoluminescent emissions in the solid state at room temperature.

1. Introduction

The construction of metal–organic CCs is of intense current interest due to their novel structures and potential applications in many fields [1–3]. As we know, construction of CCs is mainly dependent on the metal centers and organic ligands. The Ag(I) ion with d^{10} closed-shell electronic configuration is famous for having pliant coordination geometries including linearity, triangle, tetrahedron and trigonal-pyramid with occasional instances of square and octahedron [4]. The structural features of the organic ligand including the relative angle and orientation of the donor groups also play an important role in controlling CCs' structures. In recent years, although heterocyclic *N*-donor ligands (such as pyridine, pyrazine, pyrimidine, and their derivatives) have been widely used in transition metal CCs as either bridging or chelating ligands [5–18], aminobenzonitrile ligands are rarely used in Ag(I) CCs due to their two weak coordinative sites, N_{amino} and N_{cyano} [19,20]. On the other hand, influence of relative positions of the donor groups of organic ligands on the assembly process has received much less attention [21–23], as a consequence, systematical investigation on this aspect becomes an urgent need. Herein, we utilized mixed-ligand strategy to construct three new Ag/aminobenzonitrile/3,5-dinitrobenzoic acid CCs ranging from 2D to 0D and discussed the influence of the relative position of amino and cyano groups of aminobenzonitrile ligands on the resulting structures.

2. Experimental

2.1. Materials and physical measurements

All the reagents and solvents employed were commercially available and used as received without further purification. Infrared spectra were recorded on a Nicolet AVATAT FT-IR330 spectrometer as KBr pellets in the frequency range 4000–400 cm^{-1}. The elemental analyses (C, H, N contents) were determined on a CE instruments EA 1110 analyzer. Photoluminescence measurements were performed on a Hitachi F-7000 fluorescence spectrophotometer with solid powder on a 1 cm quartz round plate.

2.2. Synthesis of compound $\{[Ag(p\text{-abn})(dnca)]\cdot H_2O\}_n$ (1)

A mixture of Ag_2O (23 mg, 0.1 mmol), *p*-abn (24 mg, 0.2 mmol) and Hdnca (42 mg, 0.2 mmol) was stirred in methanol-ethanol mixed solvent (6 mL, v/v: 1/1). Then aqueous NH_3 solution (25%, 1 mL) was dropped into the mixture to give a clear solution under ultrasonic treatment. The resultant solution was allowed to evaporate slowly in darkness at room temperature for several days to give yellow crystals of **1** (Yield: 46%, based on silver). Anal. Calc. (found) for $AgC_{14}H_{11}N_4O_7$: C, 36.95 (36.94); H, 2.44 (2.34); N,

---

* Corresponding author.
E-mail address: rbhuang@xmu.edu.cn (R.-B. Huang).

0022-2860/$ - see front matter © 2011 Elsevier B.V. All rights reserved.
doi:10.1016/j.molstruc.2011.01.035

12.31 (12.25)%. IR (KBr): ν(cm^{-1}) = 3477 (m), 3372 (s), 3213 (w), 3101 (w), 3082 (w), 2214 (m), 1624 (s), 1603 (m), 1581 (m), 1533 (s), 1451 (w), 1382 (m), 1344 (s), 1326 (m), 1176 (m), 1073 (w), 918 (w), 839 (w), 830 (w), 798 (w), 733 (m), 721 (s), 547 (w).

2.3. Synthesis of compound {[Ag(o-abn)(dnca)]·H_2O}$_n$ (**2**)

The synthesis of **2** was similar to that of **1**, but with *o*-abn (24 mg, 0.2 mmol) in place of *p*-abn. Yellow crystals of **2** were obtained in 53% yield (based on silver). They were washed with a small volume of cold ethanol. Anal. Calc. (found) for $AgC_{14}H_{11}N_4O_7$: C, 36.95 (36.52); H, 2.44 (2.44); N, 12.31 (12.20)%. IR (KBr): ν(cm^{-1}) = 3459 (m), 3367 (m), 3102 (m), 3091 (m), 2209 (m), 1623 (s), 1581 (m), 1569 (m), 1534 (s), 1494 (m), 1456 (m), 1381 (s), 1344 (s), 1265 (m), 1161 (w), 1073 (m), 935 (w), 918 (m), 798 (m), 747 (m), 733 (s), 721 (s), 521 (w), 494 (m).

2.4. Synthesis of compound {[Ag(m-abn)$_4$)]·(dnca)·H_2O}$_n$ (**3**)

The synthesis of **3** was similar to that of **1**, but with *m*-abn (24 mg, 0.2 mmol) in place of *p*-abn. Yellow crystals of **3** were obtained in 68% yield (based on silver). They were washed with a small volume of cold ethanol. Anal. Calc. (found) for $AgC_{35}H_{29}N_{10}O_7$: C, 51.93(49.11); H, 3.61 (3.29); N, 17.30 (16.52)%. IR (KBr): ν(cm^{-1}) = 3401 (s), 3332 (m), 3226 (m), 3102 (m), 3092 (m), 2233 (m), 1624 (s), 1599 (s), 1581 (s), 1532 (s), 1591 (m), 1478 (w), 1447 (m), 1381 (m), 1345 (s), 1323 (m), 1294 (m), 1168 (w), 1157 (w), 1073 (m), 993 (w), 935 (w), 918 (m), 863 (m), 789 (m), 733 (m), 722 (s), 686 (m), 523 (m), 477 (m).

3. X-ray crystallography

Single crystals of the compounds **1–3** with appropriate dimensions were mounted on a glass fiber and used for data collection. Data were collected on a Bruker-AXS CCD diffractometer equipped with a graphite-monochromated Mo Kα radiation source (λ = 0.71073 Å) for **1**, and a Rigaku R-AXIS RAPID Imaging Plate single-crystal diffractometer equipped with a graphite-monochromated Mo Kα radiation source (λ = 0.71073 Å) for **2** and **3**. The crystal structures were solved by direct methods and refined with the full-matrix least-squares technique on F^2 using the SHELXS-97 and SHELXL-97 programs [24,25]. The positions of the water H atoms were refined with the O—H bond length restrained to 0.85 Å. The crystallographic details of **1–3** are summarized in Table 1. Selected bond lengths and angles for **1–3** are collected in Table 2. The hydrogen bond geometries for **1–3** are shown in Table 3.

4. Results and discussion

4.1. Syntheses and IR

The syntheses of compounds **1–3** were carried out in the darkness to avoid photodecomposition. The infrared spectra and

Table 2
Selected bond distances (Å) and angles (°) for **1–3**.

Complex **1**			
Ag1—O1	2.214 (2)	Ag1—N1	2.545 (3)
Ag1—O2^{i}	2.216 (2)	Ag1—Ag1^{i}	2.9262 (6)
Ag1—N2^{ii}	2.435 (3)		
O1—Ag1—O2^{i}	154.24 (9)	O1—Ag1—N1	115.19 (9)
O1—Ag1—N2^{ii}	95.49 (10)	O2^{i}—Ag1—N1	87.10 (9)
O2^{i}—Ag1—N2^{ii}	95.33 (9)	N2^{ii}—Ag1—N1	94.68 (10)
Symmetry codes: (i) $-x+1, -y+2, -z+1$; (ii) $-x+1, y+1/2, -z+1/2$.			
Complex **2**			
Ag1—O2^{i}	2.258 (2)	Ag1—N1	2.532 (3)
Ag1—O1	2.287 (3)	Ag1—Ag1^{i}	2.9441 (8)
Ag1—N2^{ii}	2.338 (3)		
O2^{i}—Ag1—O1	154.17 (11)	O2^{i}—Ag1—N1	100.39 (11)
O2^{i}—Ag1—N2^{ii}	109.07 (13)	O1—Ag1—N1	95.95 (11)
O1—Ag1—N2^{ii}	89.26 (13)	N2^{ii}—Ag1—N1	94.60 (13)
Symmetry codes: (i) $-x+1, -y+1, -z$; (ii) $x+1, y, z$.			
Complex **3**			
Ag1—N5	2.327 (3)	Ag1—N1	2.372 (3)
Ag1—N3	2.338 (3)	Ag1—N8	2.452 (3)
N5—Ag1—N3	123.18 (10)	N5—Ag1—N8	107.74 (10)
N5—Ag1—N1	107.35 (9)	N3—Ag1—N8	97.31 (11)
N3—Ag1—N1	122.21 (9)	N1—Ag1—N8	91.78 (11)

Table 1
Crystallographic data for complexes **1–3**.

Complexes	1	2	3
Formula	$AgC_{14}H_{11}N_4O_7$	$AgC_{14}H_{11}N_4O_7$	$AgC_{35}H_{29}N_{10}O_7$
M_r	455.14	455.14	809.55
Crystal system	Monoclinic	Monoclinic	triclinic
Space group	*P*2(1)/c	*P*2(1)/n	*P*-1
a (Å)	10.2297 (18)	6.6015 (13)	7.6256 (15)
b (Å)	6.5434 (11)	7.5135 (15)	14.919 (3)
c (Å)	22.729 (4)	32.483 (7)	17.290 (3)
α (deg)	90.00	90.00	114.89 (3)
β (deg)	99.639 (3)	91.03 (3)	96.42 (3)
γ (deg)	90.00	90.00	96.94 (3)
Z	4	4	2
V (Å^3)	1499.9 (5)	1610.9 (6)	1742.1 (6)
D_c (g cm^{-3})	2.016	1.877	1.543
μ(mm^{-1})	1.396	1.300	0.643
F (0 0 0)	904	904	824
No. of unique reflns	2619	2821	6091
No. of obsd reflns [$I > 2\sigma(I)$]	2542	2471	5355
Parameters	235	235	482
GOF	1.158	1.131	1.163
Final *R* indices [$I > 2\sigma(I)$][a,b]	R_1 = 0.0303 wR_2 = 0.0826	R_1 = 0.0301 wR_2 = 0.0761	R_1 = 0.0324 wR_2 = 0.0786
R indices (all data)	R_1 = 0.0318 wR_2 = 0. 0837	R_1 = 0.0365 wR_2 = 0.0838	R_1 = 0.0397 wR_2 = 0.1004
Largest difference peak and hole (e Å^{-3})	0.522 and −0.547	0.851 and −0.497	0.701 and −0.790

[a] $R_1 = \Sigma||F_o| - |F_c||/\Sigma|F_o|$.

[b] $wR_2 = [\Sigma w(F_o^2 - F_c^2)^2/\Sigma w(F_o^2)^2]^{0.5}$.

Table 3
The hydrogen bond geometries for **1**–**3**.

*Complex **1***				
D—H···*A*	*D*—H	H···*A*	*D*···*A*	*D*—H···*A*
N1—H1A···O5^{iii}	0.92	2.17	3.027 (4)	155
N1—H1B···O6^{iv}	0.92	2.29	3.118 (4)	149
Symmetry codes: (iii) $x + 1$, y, z; (iv) $-x$, $-y + 1$, $-z + 1$.				
*Complex **2***				
D—H···*A*	*D*—H	H···*A*	*D*···*A*	*D*—H···*A*
N1—H1A···O1W^{iii}	0.92	2.31	3.151 (9)	153
O1W—H1WA···O1	0.85	1.92	2.758 (7)	167
Symmetry code: (iii) x, $y + 1$, z.				
*Complex **3***				
D—H···*A*	*D*—H	H···*A*	*D*···*A*	*D*—H···*A*
N1—H1B···O2^{i}	0.92	2.08	2.988 (3)	170
N3—H3A···O2^{iii}	0.92	2.03	2.942 (3)	172
N5—H5A···O1W^{iii}	0.92	2.17	2.989 (4)	149
N5—H5B···O1W^{ii}	0.92	2.06	2.913 (4)	155
O1W—H1WA···O2^{iv}	0.85	2.04	2.866 (3)	165
O1W—H1WB···O1	0.85	1.90	2.738 (3)	169
Symmetry codes: (i) $x + 1$, $y + 1$, z; (ii) $-x + 1$, $-y + 2$, $-z$; (iii) x, $y + 1$, z; (iv) $-x$, $-y + 1$, $-z$.				

elemental analyses of **1–3** are fully consistent with their formations. Their IR spectra exhibit strong absorptions centered at ~3400 to ~3100 cm^{-1} corresponding to asymmetric and symmetric N—H stretching bands of amino group as well as the O—H stretching vibration of the water molecule. The peak at ~2200 cm^{-1} can be assigned to the characteristic vibrations of C≡N of the cyano group. Strong characteristic bands of carboxylic group are observed in the range of ~1620–1580 cm^{-1} for asymmetric vibrations and ~1480 cm^{-1} for symmetric vibrations, respectively.

4.2. Crystal structures

4.2.1. Crystal structure of {[Ag(p-abn)(dnca)]·H_2O}$_n$ (**1**)

X-ray single-crystal analysis reveals that **1** crystallizes in the monoclinic space group *P*2(1)/*c* whose asymmetric unit contains one Ag(I) ion, one *p*-abn ligand, one dnca anion and one lattice water molecule. As shown in Fig. 1a, the center silver ion is coordinated by two nitrogen atoms (one N_{amino} and one N_{cyano}) from two different *p*-abn ligands and two oxygen atoms from two carboxylate groups to form a distorted tetrahedral coordination geometry

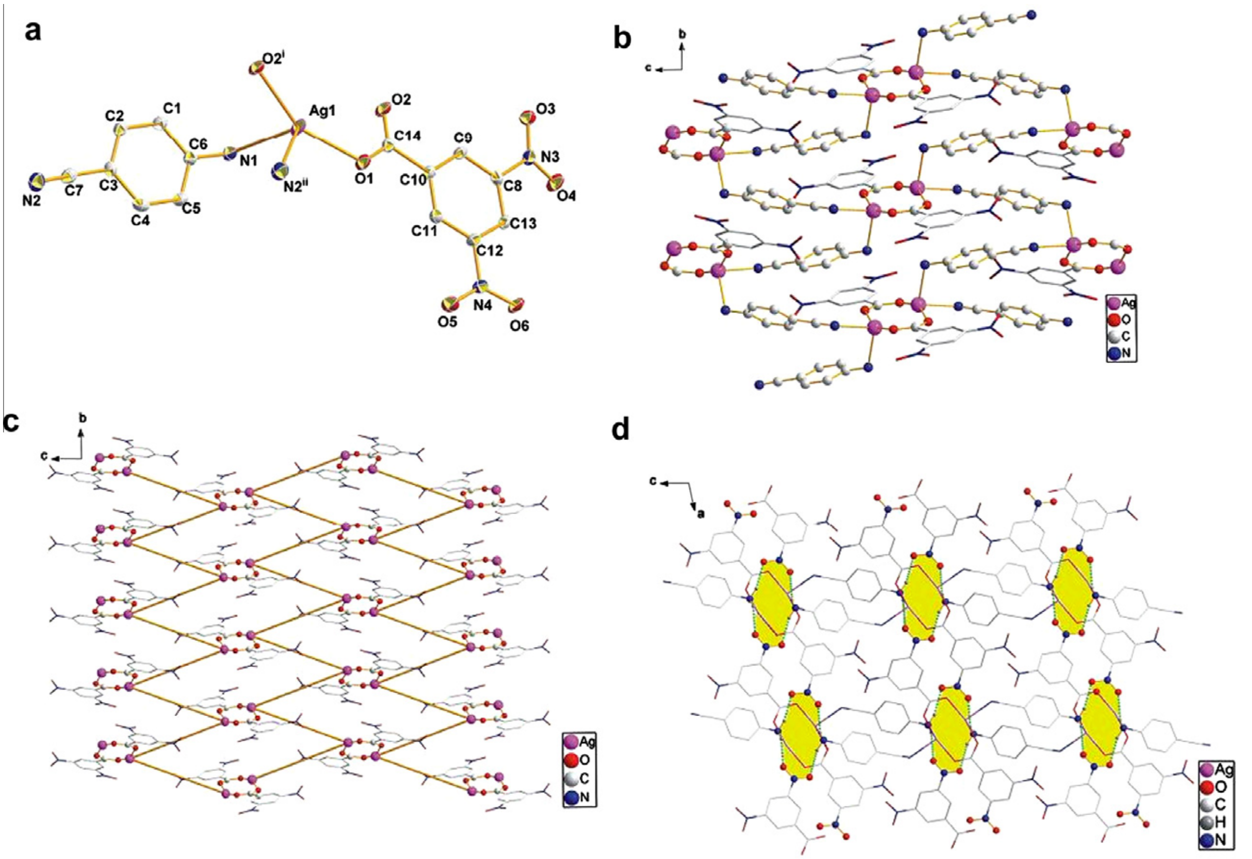

Fig. 1. (a) The coordination environment of the Ag(I) ion and the linkage modes of ligands in **1** with 50% thermal ellipsoid probability. Water molecule and hydrogen atoms are omitted for clarity. (b) The 2D network viewed along *a* axis. (c) Simplified 2D stair-shaped network. (d) The hydrogen bonds of adjacent network. (Symmetry codes: (i) $-x + 1$, $-y + 2$, $-z + 1$; (ii) $-x + 1$, $y + 1/2$, $-z + 1/2$.).

[Ag1—N1 = 2.545(3), Ag1—N2^{ii} = 2.435(3), Ag1—O1 = 2.214(2), Ag1—O2^{i} = 2.216(2) Å] without consideration of Ag···Ag interaction. Notably, the Ag—N bond lengths in **1** are obviously longer than other reported Ag—N$_{heterocycle}$ bond [26–36] suggesting N$_{amino}$ and N$_{cyano}$ atoms are both weaker electron donor compared to N$_{heterocycle}$ atoms. The distortion of the tetrahedron can be indicated by the calculated value of the τ_4 parameter introduced by Houser [37] to describe the geometry of a four-coordinate metal system, which is 0.64 for Ag1 (for perfect tetrahedral geometry, $\tau_4 = 1$). It is noteworthy that a pair of oppositely arranged μ_2-dnca ligands bind two Ag(I) ions (average Ag-O = 2.215(4) Å) with a syn-syn mode to form a [Ag$_2$(dnca)$_2$] eight-membered ring subunit. The intra-subunit shortest Ag···Ag contact is 2.9262(6) Å, which is obviously shorter than the twice the van der Waals radius of Ag(I) [38] and indicates so-called argentophilic interaction [39–43]. This distance is shorter than those (3.116(1) and 3.286(2) Å) found in two reported infinite molecular ladders ([Ag(bipy)X], $X = H_2PO_4^-$ and $MeCO_2^-$) [44] and those (2.970(2)–3.312(1) Å) found in other Ag(I) coordination polymers with pyridyl ligands [45,46]. On the other hand, the binuclear Ag(I) units were linked to form an infinite 2D network by *p*-abn ligands with opposite arrangement in a μ_2-η^1:η^1 bridging mode (Fig. 1b). Six Ag(I) ions as nodes are connected *via* four μ_2-*p*-abn ligands and two Ag···Ag contacts to form a ladder-like hexagon, then the 2D structure can be simplified into a stair-shaped network constructed by this kind of hexagon (Fig. 1c).

As shown in Fig. 1d, between the adjacent networks, the amino group (donor) of *p*-abn is hydrogen bonded to two oxygen atoms of two different nitro groups with the N$_{amino}$···O$_{nitro}$ distances of 3.027(4) and 3.118(4) Å to form a $R_4^4(12)$ hydrogen bond motif [47]. This kind of hydrogen bond motif extends the 2D network into a 3D supramolecular framework. (Symmetry codes: (i) $-x+1$, $-y+2$, $-z+1$; (ii) $-x+1$, $y+1/2$, $-z+1/2$.).

4.2.2. Crystal structure of {[Ag(*o*-abn)(dnca)]·H$_2$O}$_n$ (**2**)

When *p*-abn is replaced by its isomer *o*-abn and react with Ag$_2$O and dnca ligand under the similar synthetic condition, a 1D chain structure is produced, which crystallizes in the monoclinic space group *P*2(1)/*n*. As shown in Fig. 2a, the asymmetric unit of **2** consists of one Ag(I) ion, one *o*-abn ligand, one dnca anion and one lattice water molecule. The crystallographically independent Ag1 ion is coordinated by two nitrogen atoms from two *o*-abn ligands and two oxygen atoms from two dnca anions to form a distorted tetrahedral coordination geometry [Ag1—N1 = 2.532(3), Ag1—N2^{ii} = 2.338(3), Ag1—O1 = 2.287(3), Ag1—O2^{i} = 2.258(2) Å] without consideration of Ag···Ag interaction, then the τ_4 parameter is 0.69 for Ag1. Similarly, a pair of μ_2-dnca ligands with opposite arrangement bind two Ag(I) ions (average Ag—O = 2.273(5) Å) with a syn-syn mode to form a [Ag$_2$(dnca)$_2$] eight-membered ring subunit. The intra-subunit shortest Ag···Ag contact is 2.9441(8) Å which is comparable to that in compound **1**. On the other hand, two oppositely arranged μ_2-*o*-abn ligands linked four Ag(I) ions from two subunits to form a [Ag$_4$(*o*-abn)$_2$] fourteen-membered ring subunit incorporating Ag···Ag interaction. Those two kinds of subunits interlock with each other to form a 1D infinite chain (Fig. 2b and c).

As shown in Fig. 2d, the lattice water molecules (acceptor and donor) interact with the amino (donor) and carboxylate (acceptor) groups through hydrogen bonds which extend the 1D chain into 2D supramolecular sheet. (Symmetry codes: (i) $-x+1$, $-y+1$, $-z$; (ii) $x+1$, y, z.).

4.2.3. Crystal structure of {[Ag(*m*-abn)$_4$)]·(dnca)·H$_2$O}$_n$ (**3**)

When using *m*-abn as *N*-donor ligand, a three-foothold shaped 0D compound **3** is obtained. It crystallizes in the triclinic space group *P*-1. The asymmetric unit of **3** consists of one Ag(I) ion, four

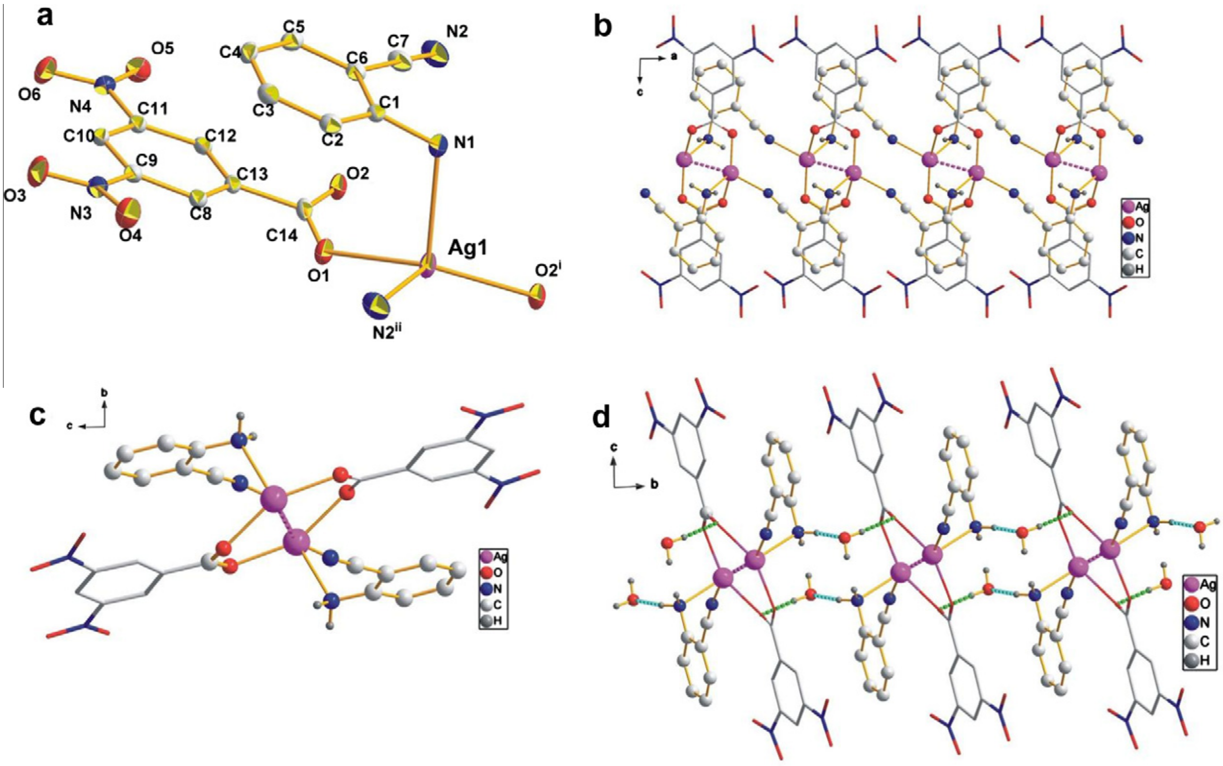

Fig. 2. (a) The coordination environment of the Ag(I) ion and the linkage modes of ligands in 2 with 30% thermal ellipsoid probability. Water molecule and hydrogen atoms are omitted for clarity. (b) The 1D chain structure viewed along *b* axis. (c) The 1D chain structure viewed along *a* axis. (d) The hydrogen bonds of adjacent chains. (Symmetry codes: (i) $-x+1$, $-y+1$, $-z$; (ii) $x+1$, y, z.).

m-abn ligands, one dnca anion and one lattice water molecule. As shown in Fig. 3a, Ag(I) ion adopts distorted $[AgN_4]$ tetrahedral geometry where one N atom comes from cyano group of a *m*-abn ligand and the rest N atoms are from the amino group of three *m*-abn ligands. The $Ag—N_{cyano}$ bond length is 2.452(3) and the $Ag—N_{amino}$ bond length fall in the range 2.327(3)–2.338(3) Å. The τ_4 parameter is 0.81 for Ag1. Different from **1** and **2**, the dnca anion does not participate in the coordination with metal center and just acts as guest counteranion in **3**.

Two symmetry-related lattice water molecules act as acceptors and are hydrogen-bonded to two amino groups to form a $R_4^2(8)$ motif (Fig. 3b). On the other hand, two symmetry-related lattice water molecules also act as donors and are hydrogen-bonded to two nitro groups to form a $R_4^4(12)$ motif. These two kinds of hydrogen bond motifs share the edges to extend the 0D complex into a 1D supramolecular chain. The average N—H···O and O—H···O distances are 2.958(12) and 2.802(6) Å. The π···π and C—H···π interactions (as shown in Table 4, average centroid···centroid distance and dihedral angle are 3.867(2) Å and 4.3°, respectively, Fig. S1 and S2, Supporting Information. $d_{C\cdots Cg} = 3.547(3)$ Å, $\theta = 163°$, Fig. S3, Supporting Information) also enhance the stability of the resulting 1D.

4.3. Influence of the relative position of amino and cyano groups of aminobenzonitrile ligands

Based on above analysis, the structural diversity of compounds **1** and **2** should be arisen from the different relative orientations of amino and cyano groups situated in the benzene ring. In **1**, *p*-abn ligand, with an angle θ [48] between the two groups of 180°, adopts *N,N'*-bidentate bridging mode to extend the $[Ag_2(dnca)_2]$ subunit to a 2D network. However, when the angle θ between the amino and cyano groups is turned from 180 to 60°, that is, *p*-abn is replaced by *o*-abn, the hindrance effect between these two groups has increased obviously, as a result, the similar $[Ag_2(dnca)_2]$ subunit of **2** cannot be extended to the 2D sheet, but only can form a 1D chain structure by coordinating with *o*-abn ligand in a *N,N'*-bidentate bridging fashion. The bond length of $Ag—N_{amino}$ and $Ag—N_{cyano}$ decreases from 2.545(3) and 2.435(3) to 2.532(3) and 2.338(3) Å. When the θ is modified to 120°, that is, *o*-abn is replaced by *m*-abn, the resulting structure of **3** is a 0D CC, at the same time, dnca only acts as guest counteranion and does not interact with the metal center. In all, different relative positions of amino and cyano groups of aminobenzonitrile ligands bring different steric effects which intensely influence their coordination modes, as a result, diverse structural motifs were formed.

4.4. Photoluminescence properties

Emissive CCs are of great current interest because of their various applications in chemical sensors, photochemistry and electroluminescent display [49,50]. Thus, the photoluminescence properties of **1–3** as well as free ligands were examined in the solid state at room temperature (Fig. 4). The *p*-abn, *o*-abn and *m*-abn ligands display photoluminescent emissions at 339, 408 and 375 nm respectively under 300 nm radiation which are probably attributed to the $\pi^* \rightarrow \pi$ transition [51–53]. The intense emission bands at 336 nm (λ_{ex} = 250 nm) for **1**, 382 nm (λ_{ex} = 300 nm) for **2** and 397 nm (λ_{ex} = 300 nm) for **3** are observed at room temperature which are similar to that of the corresponding aminobenzonitrile ligands. Consideration of weak emissive essence of Hdnca ligand [54], the photoluminescence of compound **1**–**3** should originate from the transitions between the energy levels of *N*-donor ligands [55].

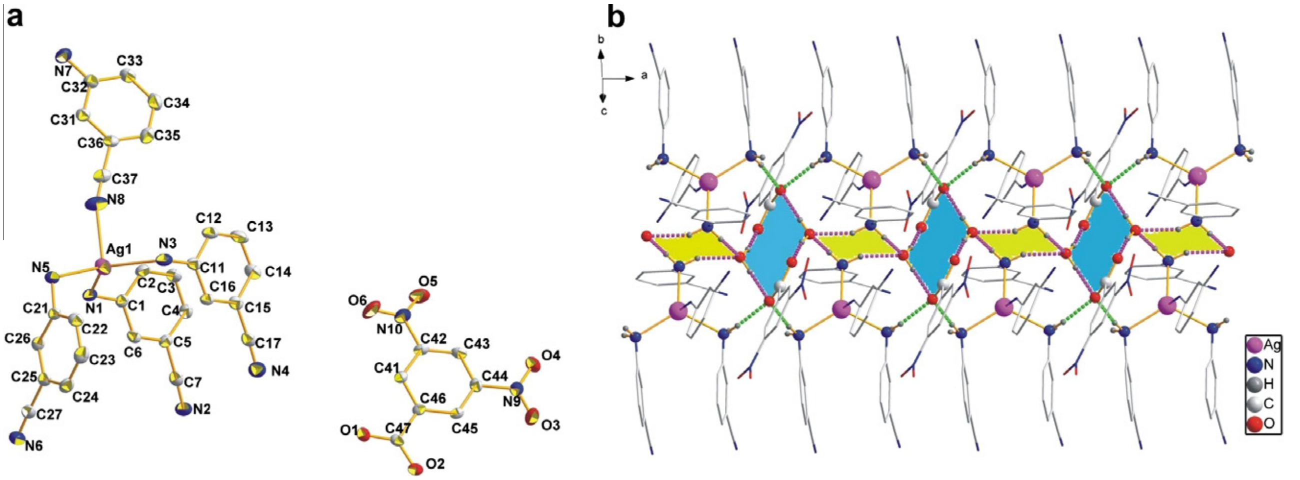

Fig. 3. (a) The coordination environment of the Ag(I) ion and the linkage modes of ligands in **3** with 50% thermal ellipsoid probability. Water molecule and hydrogen atoms are omitted for clarity. (b) The 1D chain structure.

Table 4
π···π and C—H···π interactions in **3**.

ring (i) → ring (j)	Cg···Cg(Å)	Dihedral angle (i,j) (°)	Cg(i) → ring (j) (Å)	Cg(j) → ring (i) (Å)	β [°]
Cg1···Cg2	3.877 (2)	7.30	3.6759 (13)	3.5505 (14)	23.67
Cg1···Cg2^{v}	3.764 (2)	7.30	3.6712 (13)	3.6035 (14)	16.80
Cg4···Cg5^{iii}	3.974 (2)	1.30	3.4273 (14)	3.4669 (13)	29.26
Cg4···Cg5^{i}	3.853 (2)	1.30	3.3675 (14)	3.4044 (13)	27.92
X-H(i) → Cg(j)	H···Cg(Å)	X-H···Cg[°]	X···Cg(Å)		
C31-H71A → Cg3^{vi}	2.63	163	3.547(3)		

Cg1: C1/C2/C3/C4/C5/C6; Cg2: C11/C12/C13/C14/C15/C16; Cg3: C21/C22/C23/C24/C25/C26; Cg4: C31/C32/C33/C34/C35/C36; Cg5: C41/C42/C43/C44/C45/C46.
Symmetry codes: (i) $x + 1, y + 1, z$; (iii) $x, y + 1, z$; (v) $x + 1, y, z$; (vi) $-x + 1, -y + 3, -z$. β = Angle Cg(i) → Cg(j) or Cg(i) → Me vector and normal to ring (i).

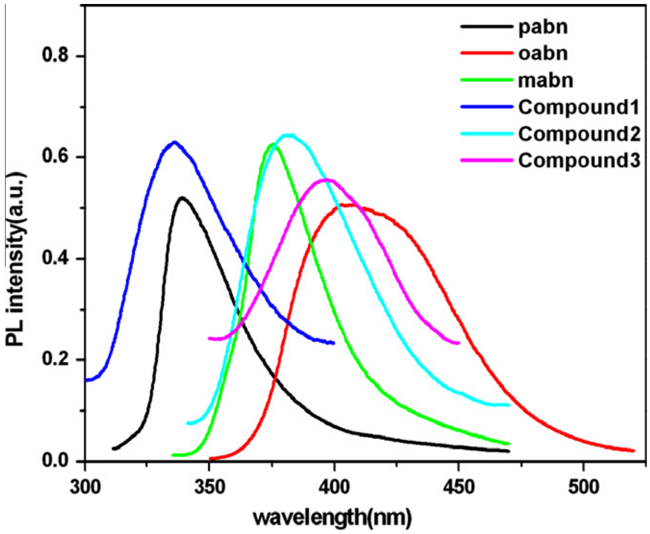

Fig. 4. Emission spectra of the abn ligands and complexes **1**–**3**.

5. Conclusions

In summary, we demonstrate the synthesis and characterization of three photoluminescent 2D, 1D, and 0D Ag(I) CCs under the ammoniacal condition. As the relative position of amino and cyano groups of aminobenzonitrile ligands changes, the dimensionality of CCs decreases from 2D to 0D which mainly results from the steric effect of substituents in this system. These results provide a way of understanding the influence of the substituents of aminobenzonitrile ligands on the resultant structures. Moreover, photoluminescent properties of three CCs are also discussed.

Acknowledgments

This work was financially supported by the National Natural Science Foundation of China (Nos. 21021061 and 21071118), 973 Project (Grant 2007CB815301) from MSTC. Dr. G.-G. Luo also thanks the Startup Package Funding of Huaqiao University (No. 10BS210) for supporting.

Appendix A. Supplementary material

Supplementary data associated with this article can be found, in the online version, at doi:10.1016/j.molstruc.2011.01.035.

CCDC 805802, 805803 and 805804 contain the supplementary crystallographic data for 1–3 respectively in this paper. These data can be obtained free of charge via http://www.ccdc.cam.ac.uk/conts/retrieving.html, or from the Cambridge Crystallographic Data Centre, 12 Union Road, Cambridge CB 21EZ, UK; fax: (+44) 1223–336-033; or e-mail: deposit@ccdc.cam.ac.uk. Supplementary data associated with this article can be found, in the online version.

References

[1] C. Janiak, Dalton Trans. (2003) 2781.
[2] N.W. Ockwig, O. Delgado-Friedrichs, M. O'Keeffe, O.M. Yaghi, Acc. Chem. Res. 38 (2005) 176.
[3] O.R. Evans, W. Lin, Acc. Chem. Res. 35 (2002) 511.
[4] D. Venkataraman, Y. Du, S.R. Wilson, P. Zhang, K. Hirsch, J.S. Moore, J. Chem. Ed. 74 (1997) 915.
[5] D. Sun, G.G. Luo, R.B. Huang, N. Zhang, L.S. Zheng, Acta Crystallogr. C65 (2009) m305.
[6] D. Sun, G.G. Luo, N. Zhang, J.H. Chen, R.B. Huang, L.R. Lin, L.S. Zheng, Polyhedron 28 (2009) 2983.
[7] D. Sun, G.G. Luo, N. Zhang, R.B. Huang, L.S. Zheng, Acta Crystallogr. C65 (2009) m418.
[8] D. Sun, G.G. Luo, N. Zhang, R.B. Huang, L.S. Zheng, Acta Crystallogr. C65 (2009) m440.
[9] D. Sun, G.G. Luo, N. Zhang, Q.J. Xu, C.F. Yang, Z.H. Wei, Y.C. Jin, L.R. Lin, R.B. Huang, L.S. Zheng, Inorg. Chem. Commun. 13 (2010) 290.
[10] D. Sun, N. Zhang, R.-B. Huang, L.-S. Zheng, Cryst. Growth Des. 10 (2010) 3699.
[11] D. Sun, G.G. Luo, N. Zhang, Z.H. Wei, C.F. Yang, Q.J. Xu, R.B. Huang, L.S. Zheng, J. Mol. Struct. 967 (2010) 147.
[12] D. Sun, H.-R. Xu, C.-F. Yang, Z.-H. Wei, N. Zhang, R.-B. Huang, L.-S. Zheng, Cryst. Growth Des. 10 (2010) 4642.
[13] C.-Y. Lin, Z.-K. Chan, C.-W. Yeh, C.-J. Wu, J.-D. Chen, J.-C. Wang, CrystEngComm 8 (2006) 841.
[14] Y.-H. Wang, K.-L. Chu, H.-C. Chen, C.-W. Yeh, Z.-K. Chan, M.-C. Suen, J.-D. Chen, Cryst. Eng. Commun. 8 (2006) 84.
[15] D. Sun, D.-F. Wang, X.-G. Han, N. Zhang, R.-B. Huang, L.-S. Zheng, Chem. Commun. 47 (2010) 746.
[16] D. Sun, C.-F. Yang, H.-R. Xu, H.-X. Zhao, Z.-H. Wei, N. Zhang, L.-J. Yu, R.-B. Huang, L.-S. Zheng, Chem. Commun. 46 (2010) 8168.
[17] D. Sun, Q.-J. Xu, C.-Y. Ma, N. Zhang, R.-B. Huang, L.-S. Zheng, Cryst. Eng. Commun. 12 (2010) 4161.
[18] D. Sun, G.G. Luo, N. Zhang, Z.H. Wei, C.F. Yang, Q.J. Xu, R.B. Huang, L.S. Zheng, Chem. Commun. 47 (2011) 1461.
[19] D. Sun, G.-G. Luo, R.-B. Huang, N. Zhang, L.-S. Zheng, Acta Crystallogr. Sect. C Cryst. Struct. Commun. C65 (2009) m305.
[20] D. Sun, Z.H. Wei, C.F. Yang, D.F. Wang, N. Zhang, R.-B. Huang, N. Zhang, L.-S. Zheng, CrystEngComm (2011), doi: 10.1039/C0CE00539H.
[21] L. Zhao, X.-L. Zhao, T.C.W. Mak, Chem.-Eur. J. 13 (2007) 5927.
[22] A. Bellusci, A. Crispini, D. Pucci, E.I. Szerb, M. Ghedini, Cryst. Growth Des. 8 (2008) 3114.
[23] K.M.-C. Wong, L.-L. Hung, W.H. Lam, N. Zhu, V.W.-W. Yam, J. Am. Chem. Soc. 129 (2007) 4350.
[24] G.M. Sheldrick, SHELXS 97: Program for Crystal Structure Solution, University of Göttingen, Germany, 1997.
[25] G.M. Sheldrick, SHELXL 97: Program for Crystal Structure Refinement, University of Göttingen, Germany, 1997.
[26] K.V. Domasevitch, P.V. Solntsev, I.A. Gural'skiy, H. Krautscheid, E.B. Rusanov, A.N. Chernega, J.A.K. Howard, Dalton Trans. (2007) 3893.
[27] I.A. Gural'skiy, D. Escudero, A. Frontera, P.V. Solntsev, E.B. Rusanov, A.N. Chernega, H. Krautscheid, K.V. Domasevitch, Dalton Trans. (2009) 2856.
[28] A.S. Degtyarenko, P.V. Solntsev, H. Krautscheid, E.B. Rusanov, A.N. Chernega, K.V. Domasevitch, New J. Chem. 32 (2008) 1910.
[29] H.C. Chen, H.L. Hu, Z.K. Chan, C.W. Yeh, H.W. Jia, C.P. Wu, J.D. Chen, J.C. Wang, Cryst. Growth Des. 7 (2007) 698.
[30] C.W. Yeh, T.R. Chen, J.D. Chen, J.C. Wang, Cryst. Growth Des. 9 (2009) 2595.
[31] I. Ilker, O.Z. Yesilel, G. Gunay, O. Buyukgungor, J. Organomet. Chem. 694 (2009) 4178.
[32] Y.O. Jang, S.W. Lee, Polyhedron 29 (2010) 2731.
[33] H.S. Huh, S.H. Kim, S.Y. Yun, S.W. Lee, Polyhedron 27 (2008) 1229.
[34] E. Guney, V.T. Yilmaz, O. Buyukgungor, Polyhedron 29 (2010) 1437.
[35] V.T. Yilmaz, S. Hamamci, S. Gumus, O. Buyukgungor, J. Mol. Struct. 794 (2006) 142.
[36] S. Hamamci, V.T. Yilmaz, W.T.A. Harrison, J. Mol. Struct. 734 (2005) 191.
[37] L. Yang, D.R. Powell, R.P. Houser, Dalton Trans. (2007) 955.
[38] A. Bondi, J. Phys. Chem. 68 (1964) 441.
[39] L. Dobrzanska, H.G. Raubenheimer, L.J. Barbour, Chem. Commun. (2005) 5050.
[40] L. Pan, E.B. Woodlock, X. Wang, K.-C. Lam, A.L. Rheingold, Chem. Commun. (2001) 1762.
[41] J.-P. Zhang, Y.-B. Wang, X.-C. Huang, Y.-Y. Lin, X.-M. Chen, Chem.-Eur. J. 11 (2005) 552.
[42] C.-M. Che, M.-C. Tse, M.C.W. Chan, K.-K. Cheung, D.L. Phillips, K.-H. Leung, J. Am. Chem. Soc. 122 (2000) 2464.
[43] E. Guney, V.T. Yilmaz, O. Buyukgungor, Inorg. Chem. Commun. 13 (2010) 563.
[44] M.-L. Tong, X.-M. Chen, S.W. Ng, Inorg. Chem. Commun. 3 (2000) 436.
[45] O.M. Yaghi, H. Li, J. Am. Chem. Soc. 118 (1996) 295.
[46] M.A. Withersby, A.J. Blake, N.R. Champness, P. Hubberstey, W.-S. Li, M. Schröder, Angew Chem., Int. Ed. Engl. 36 (1997) 2327.
[47] J. Bernstein, R.E. Davis, L. Shimoni, N.-L. Chang, Angew Chem., Int. Ed. Engl. 34 (1995) 1555.
[48] M. Eddaoudi, J. Kim, D. Vodak, A. Sudik, J. Wachter, M. O'Keeffe, O.M. Yaghi, Proc. Natl. Acad. Sci. USA 99 (2002) 4900.
[49] Y.R. Liu, L. Li, T. Yang, X.W. Yu, C.Y. Su, CrystEngComm 11 (2009) 2712.
[50] G.D. Santis, L. Fabbrizzi, M. Licchelli, A. Poggi, A. Taglietti, Angew Chem. Int. Ed. Engl. 35 (1996) 202.
[51] A. Thirumurugan, S. Natarajan, Dalton Trans. (2004) 2923.
[52] S.Q. Liu, T. KurodaSowa, H. Konaka, Y. Suenaga, M. Maekawa, T. Mizutani, G.L. Ning, M. Munakata, Inorg. Chem. 44 (2005) 1031.
[53] D. Sun, N. Zhang, Q.J. Xu, G.G. Luo, R.B. Huang, L.S. Zheng, J. Mol. Struct. 970 (2010) 134.
[54] W.J. Chen, Y. Wang, C. Chen, Q. Yue, H.M. Yuan, J.S. Chen, S.N. Wang, Inorg. Chem. 42 (2003) 944.
[55] F.-F. Li, J.-F. Ma, J. Yang, H.-Q. Jia, N.-H. Hu, J. Mol. Struct. 787 (2006) 106.